energy&fuels

Article

pubs.acs.org/EF

# Simulation of a Non-isothermal Industrial Hydrotreating Reactor Using Simulink

Ali Fooladi Toosi, Mohammad Sadegh Samie, Ali Dashti,* and Mahmud Atarian Shandiz

Chemical Engineering Department, Faculty of Engineering, Ferdowsi University of Mashhad, Post Office Box 9177948944, Mashhad, Iran

**ABSTRACT:** A steady-state three-phase heterogeneous model was applied for simulation of a vacuum gas oil (VGO) hydrotreating reactor in both pilot and industrial plants under non-isothermal conditions. Three main reactions, including hydrodesulfurization (HDS), hydrodearomatization (HDA), and hydrodenitrogenation (HDN), were considered, and various kinetic models were evaluated to justify the commercial reactor predictions. The influence of important operating variables, such as feed American Petroleum Institute (API) gravity, temperature, pressure, and liquid hourly space velocity (LHSV), were studied. Evaluation of simulated results showed that component concentration profiles are very close in liquid and solid phase and the model can be renewed to a pseudo-two-phase model. Thus, the differential-algebraic equations (DAEs) were converted to particularly stiff ordinary differential equations (ODEs) and solved simultaneously with the Simulink toolbox in MATLAB. The simulation was validated by pilot- and industrial-plant hydrotreater data with good agreement. With the implementation of the hydrotreater simulation in the Simulink well, the dynamic behavior studies are simplier and easier for any commercial hydrotreating reactor.

## 1. INTRODUCTION

Nowadays, crude oil is still the most important world energy source for clean fuel supplement. Available crude oils becoming more and more heavier makes refining more difficult than ever. Furthermore, the increasing demand for high-valuable products, such as gasoline and middle distillates, and more strict environmental rules dictates refiners to maximize the product quality and reduce more impurity contents. The catalytic hydrotreating (HDT) process is widely applied in the petroleum refinery industry to upgrade heavy oils and remove impurities, such as sulfur, nitrogen, oxygen, metal-containing compounds, as well as polynuclear aromatics. To maximize the product quality yield, the study of the effect of process conditions on HDT is necessary.[1−5]

Dependent upon the feed type and the desired product quality, the name of the process will change. In the case of naphtha, where sulfur is the main undesirable heteroatom, the process is called hydrodesulfurization (HDS). HDT is used for straight-run gas oil, and the hydrodemetallization (HDM) process is used for heavy oils. A hydrocracking process is used when a change in the molecular weight of the feed is purposed. Selection of the process type directly depends upon the amount of impurity content and the levels of conversion required.[6]

In ages, various residue hydroconversion processes were developed and commercially employed using a fixed bed, moving bed, ebullated bed, slurry bed, or combination. In the literature, the typical operating conditions of these reactors are presented. The deactivation rate of the catalyst is the main aspect for selecting the required process type. Now, most of the HDT reactors are a multiphase catalytic fixed bed classified to co-current and counter-current gas−liquid flow trickle beds.[7−10]

Korsten and Hoffmann developed a well-known plug-flow reactor model for the HDS, which their model has been the basis for the next studies.[11] Matos and Guirardello have presented another model to describe the hydrocracking process.[12] Possibly, Chowdhury et al.[13] accounted the hydrodearomatization (HDA) reaction in HDT modeling and simulation of diesel for the first time. Reaction kinetics dependence of the hydrocracking process with the catalyst type was investigated by Marafi et al.[14] Rodriguez and Ancheyta developed the model for hydrodenitrogenation (HDN), HDA, and HDM reactions.[6] Mederos et al. described a dynamic model for HDT and considered HDS, HDN, and HDA reactions.[15]

Murali et al.[9] carried out an experimental HDT process in a microreactor using a CoMo-type catalyst and developed a kinetic model with HDS and HDA reactions to evaluate a commercial reactor. They used different orders of reaction in proposed kinetic rates of HDS and HDA. However, the type of catalyst used in our simulation is similar to the catalyst by Murali et al.,[9] but the predicted results of the industrial reactor are not confirmed well by those kinetic models.

Alvarez et al. developed a model for hydroprocessing of heavy oil and studied the quench effect on the exit product.[16,17] Chen et al.[18] applied HDS and HDA reactions for modeling and simulation of a commercial HDT reactor based on kinetic models by Korsten and Hoffmann[11] and Chowdhury et al.[13] They considered vapor−liquid equilibrium (VLE) effects and indicated the significance of VLE in simulation results. However, the feed gravity is determinant in accounting for the VLE effect. A heavier feed needs a higher severity as well as a higher temperature and pressure; thus, less vapor phase content can be present in the system to observe VLE effects. Jarullah et al. have developed a model for the HDS of heavy

**Received:** April 1, 2014
**Revised:** June 13, 2014
**Published:** June 13, 2014

   dx.doi.org/10.1021/ef500701q | *Energy Fuels* 2014, 28, 4828−4834

**Table 1. Applied Correlations for the HDT Reactor Model Equations[11]**

| parameter | correlation |
|---|---|
| specific surface area | $a_S = \frac{6}{d_p}(1-\varepsilon)$ |
| oil density | $\rho(p,T) = \rho_0 + \Delta\rho_p - \Delta\rho_T$ |
| | $\Delta\rho_p = [0.167 + 16.181 \times 10^{-0.0425\rho_0}]\left[\frac{p}{1000}\right] - 0.01[0.299 + 263 \times 10^{-0.0603\rho_0}]\left[\frac{p}{1000}\right]^2$ |
| | $\Delta\rho_T = [0.0133 + 152.4(\rho_0 + \Delta\rho_p)^{(-2.45)}][T-520] - [8.1 \times 10^{-6} - 0.0622 \times 10^{-0.764(\rho_0+\Delta\rho_p)}][T-520]^2$ |
| oil viscosity | $\mu = 3.141 \times 10^{10}(T-460)^{-3.444}[\log_{10}(\mathrm{API})]^a$ |
| | $a = 10.313[\log_{10}(T-460)] - 36.447$ |
| oil heat capacity[a] | $C_p^L = 4.1868\left(\frac{0.415}{\sqrt{\rho_L^{15.6}}} + 0.0009[T-288.15]\right)$ |
| Henry coefficient | $H = \frac{v_N}{\lambda_i \rho_L}$ |
| solubility of $H_2$ | $\lambda_{H_2} = a_0 + a_1 T + a_2\frac{T}{\rho_{20}} + a_3 T^2 + a_4\frac{1}{\rho_{20}}$ |
| | $a_0 = -0.559729 \quad a_1 = -0.42947 \times 10^{-3}$ |
| | $a_2 = 3.07539 \times 10^{-3}$ |
| | $a_3 = 1.94593 \times 10^{-3} \quad a_4 = 0.835783$ |
| solubility of $H_2S$ | $\lambda_{H_2S} = \exp(3.6670 - 0.008470T)$ |
| molecular diffusivity | $D_i^L = 8.93 \times 10^{-8}\frac{v_L^{0.267}}{v_i^{0.433}}\frac{T}{\mu_L}$ |
| liquid molar volume | $v = 0.285 v_c^{1.048}$ |
| critical specific volume[b] | $v_c^m = 6.2 \times 10^{10}[\exp(-7.58 \times 10^{-3}T_b - 28.5524\mathrm{SG} + 1.172 \times 10^{-2}T_b\mathrm{SG})] T_b^{1.20493}\mathrm{SG}^{17.2074}$ |
| gas–liquid mass-transfer coefficient | $\frac{k_i a_L}{D_i^L} = 7\left(\frac{G_L}{\mu_L}\right)^{0.4}\left(\frac{\mu_L}{\rho_L D_i^L}\right)^{0.5}$ |
| liquid–solid mass-transfer coefficient | $\frac{k_i^S}{D_i^L a_S} = 1.8\left(\frac{G_L}{a_S\mu_L}\right)^{0.5}\left(\frac{\mu_L}{\rho_L D_i^L}\right)^{1/3}$ |

[a]Taken from ref 28. [b]Taken from ref 29.

crude oil.[19] Recently, Alvarez and Ancheyta have studied on the start of run problems and represented optimum conditions for the dynamic state of hydroprocessing.[20]

To solve the governing differential equations of the modeling, different software was used. Rodriguez et al.[21] and Jimenez et al.[22] used MATLAB software, whereas Mederos et al.[23,24] used FORTRAN language and Jarullah et al.[25,26] used gPROMS for solving the model differential equations.

In this study, we have used the MATLAB Simulink toolbox for modeling and simulation of the non-isothermal trickle-bed HDT reactor in both pilot and industrial scale. The flexibility and ability for solving differential equations with different mathematical methods in the shortest possible time are some advantages of this toolbox. Model validation has been carried out in comparison to pilot data taken from the literature[11] and industrial data.[27] As stated by Rodrıguez and Ancheyta,[6] "because kinetic information was taken from different sources, in which the operating conditions, the type of catalyst and feed, and the experimental setup, among other factors, are also different, it is almost impossible to have an exact representation of experimental data generated in other reaction systems, and recalculation of kinetic parameter values is mandatory" in the presented model, kinetic parameters were re-evaluated because of different catalyst type, feed, and operating conditions. In most HDT process simulations, only the HDS reaction is considered. There are a few studies[6,15] considering the three important reactions, including HDS, HDN, and HDA, together. In our study, these three reactions are considered.

The predicted results showed good agreement with mentioned experimental data. In this simulation, the linear increasing temperature gradient obtained along the reactor bed emphasizes the necessity of using quench streams.


dx.doi.org/10.1021/ef500701q | Energy Fuels 2014, 28, 4828–4834

## 2. MODELING AND SIMULATION OF THE HDT REACTOR

First, the well-known three-phase plug-flow reactor model was applied for the HDT modeling.[11] However, the obtained results of our simulation showed that the liquid- and solid-phase concentration profiles are very close on the catalyst surface. Thus, when mass-transfer resistances between liquid and solid phases are neglected, the initial trickle-bed model converted to a pseudo-two-phase plug-flow reactor model. The model considers mass transfer at the gas−liquid and liquid−solid interfaces and involves correlations to predict mass-transfer coefficients, gas solubilities, and specification of hydrocarbon feedstock, as shown in Table 1. The model verification is well-done by pilot-scale data reported by Korsten and Hoffmann.[11] Then, the validated model is used to simulate industrial-plant data, as presented in Table 2.[27] Simulation results showed very good agreement with industrial data.

**Table 2. Physical and Chemical Properties of the Feedstock for the Industrial HDT Reactor[27]**

| characteristic | value | unit |
|---|---|---|
| density at 15.6 °C | 0.865 | g/cm$^3$ |
| molecular weight | 245 | |
| simulated distillation | | |
| IBP | 255 | °C |
| 10 vol % | 278 | °C |
| 30 vol % | 297 | °C |
| 50 vol % | 312 | °C |
| 70 vol % | 329 | °C |
| 90 vol % | 360 | °C |
| FBP | 387 | °C |
| mean average boiling point | 310.5 | °C |
| sulfur | 1.34 | wt % |
| total nitrogen | 360 | wppm |
| total aromatics | 15.6 | wt % |

The industrial hydrotreater is dimensioned with an internal diameter of the reactor being 2.9 m and a capacity of the catalyst for loading being 72.63 m$^3$. Table 2 shows the physical and chemical properties of the feedstock. Commercial Co−Mo supported on alumina was used. The feed stream is treated under the following operating conditions: pressure, 5.17 MPa; temperature, 345 °C; liquid hourly space velocity (LHSV), 2.3 h$^{-1}$; and $H_2$/HC ratio, 163 (Nm$^3$/m$^3$).[27]

The main assumptions for the modeling simplification are as follows: (1) The one-dimensional steady-state operation with no pressure drop is considered. (2) No catalyst deactivation happened. (3) Mass-transfer resistance in the gas side of the gas−liquid interface is negligible. (4) A pseudo-two-phase model instead of a three-phase model was applied. Therefore, the differential-algebraic equations (DAEs) were converted to particular stiff ordinary differential equations (ODEs). (5) Vapor pressure for hydrocarbons is negligible. (6) There are no concentration gradients in the solid phase because of slowness of the reaction. (7) Gas and liquid velocities are constant through the reactor.

The reactor model considers the main reactions, such as HDS, HDN, and HDA. There is no reaction in the gas phase, and all of the reactions take place only on the catalyst surface. Thus, the following equation states a change in the molar gas flow rate of the gaseous compound in the gas phase:

$$\frac{dP_i}{dz} = k_i^L a_L \frac{RT}{u_G}[C_i^L] - k_i^L a_L \frac{RT}{u_G}\frac{1}{H_i}[P_i^G] \quad (1)$$

where $i$ = $H_2$ or $H_2S$. The mass balance equation of gaseous compounds in the liquid phase is

$$\frac{dC_i^L}{dz} = \frac{k_i^L a^L}{u_L}\left[\frac{P_i^G}{H_i} - C_i^L\right] + \frac{\rho_B \eta_l}{u_L} r_{HDS} \quad (2)$$

where $i$ = $H_2$ or $H_2S$. The mass balance equation of organic compounds in the liquid phase can be written as

$$\frac{dC_i^L}{dz} = \frac{\rho_B \eta_j}{u_L} r_j \quad (3)$$

where $i$ = S, N, or Ar and $j$ = HDS, HDN, or HDA. The energy balance equation to predict temperature profile along the reactor is

$$\frac{dT}{dz} = \frac{\rho_B}{(C_{P_L} u_L \rho_L + C_{P_G} u_G \rho_G)} \sum_{j=1}^{3} r_j \eta_j (-\Delta H_j) \quad (4)$$

The rate of the HDS reaction was described by the Langmuir−Hinshelwood model as[11]

$$r_{HDS} = k_{app} \frac{[C_S^S][C_{H_2}^L]^{0.45}}{(1 + K_{H_2S}[C_{H_2S}^L])^2} \quad (5)$$

The HDN reaction rate was modeled by[25]

$$r_{HDN} = k_{HDN}[C_N^L]^{1.672}[C_{H_2}]^{0.3555} \quad (6)$$

The reaction rate of HDA reported by Mederos et al.[15] was applied here

$$r_{HDA} = k_f[P_{H_2}^G][C_{Ar}^L] - k_r(1 - C_{Ar}^L) \quad (7)$$

The kinetic parameters used here were taken from different sources in the literature, as shown in Table 3. The model reactor is implemented in the Simulink toolbox of MATLAB software R2013. A part of the procedure is presented in Figure 1.

## 3. RESULTS AND DISCUSSION

First, we used the Korsten and Hoffmann experimental data[11] to validate our modeling and simulation results. The component concentration profiles through the pilot reactor bed are shown in Figures 2 and 3. As expected, the S concentration decreases and the $H_2S$ partial pressure increases. The reaction rate decreases along the reactor, which causes a steep gradient at the early stage of the reactor and a slight gradient at the late stage of the reactor. As observed in Figure 2, presented results predict very good conformity between the

**Table 3. Main Kinetic Parameters for the HDT Reactor Model[15]**

| reaction | $E_A$ (J/mol) | $K_0$ | $\Delta H$ (J/mol) |
|---|---|---|---|
| HDS | 131993 | $4.266 \times 10^9$ cm$^3$ g$^{-1}$ s$^{-1}$ (cm$^3$ mol$^{-1}$)$^{0.45}$ | 251 |
| HDN[a] | 71775.5 | $2.85 \times 10^7$ (mol cm$^{-3}$)$^{-0.672}$ (cm$^3$ g$^{-1}$ s$^{-1}$) (mol cm$^{-3}$)$^{-0.355}$ | 64.85 |
| HDA | | | 255 |
| forward | 121400 | $1.041 \times 10^5$ s$^{-1}$ MPa$^{-1}$ | |
| reverse | 186400 | $8.805 \times 10^9$ s$^{-1}$ | |

[a]Taken from ref 23.


dx.doi.org/10.1021/ef500701q | Energy Fuels 2014, 28, 4828−4834

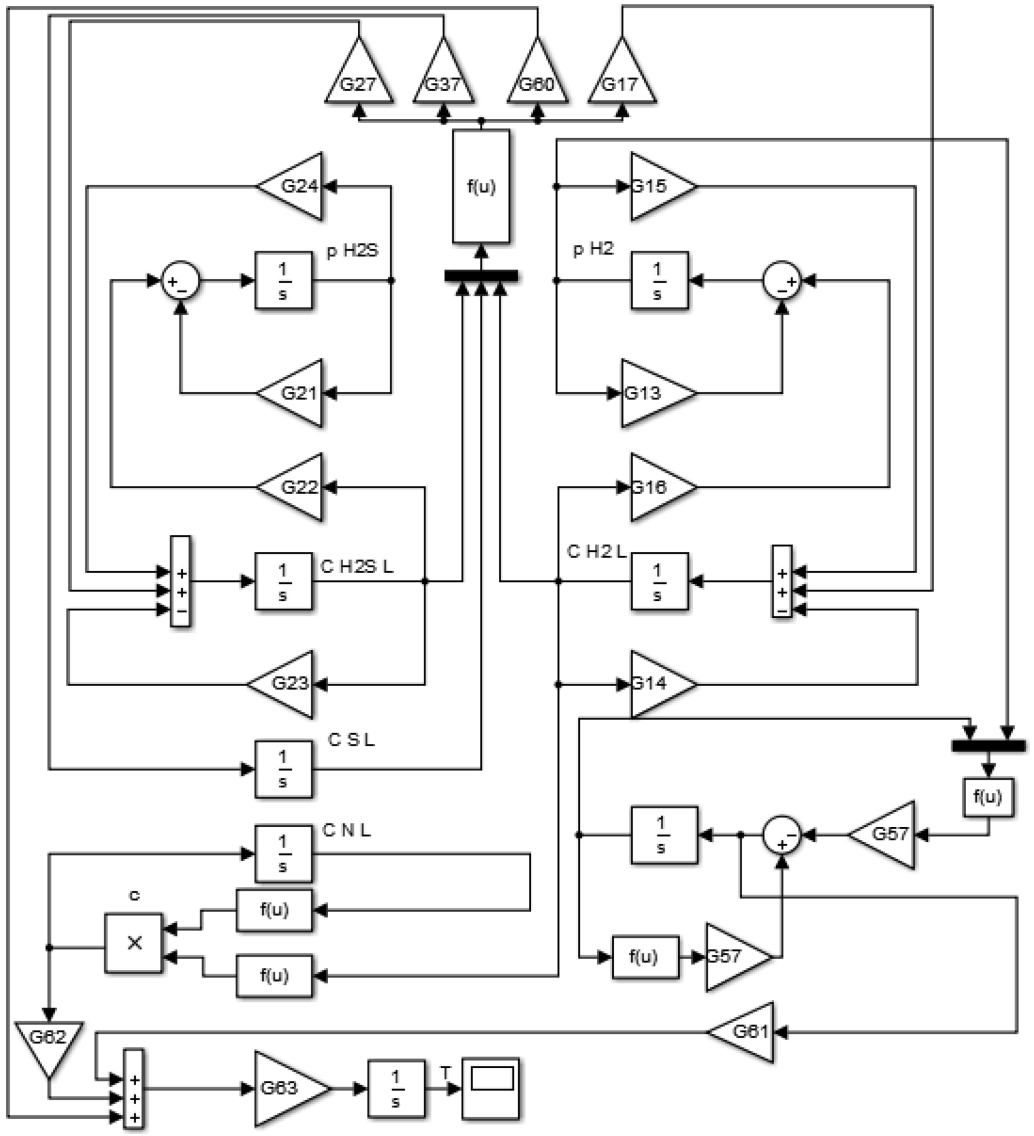


**Figure 1.** Part of the Simulink procedure scheme for the presented HDT simulation.

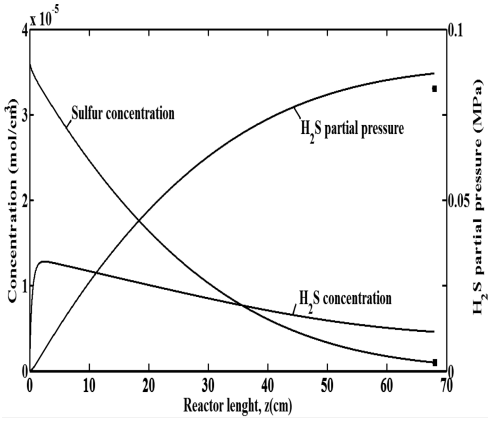


**Figure 2.** Profiles of the sulfur concentration and $H_2S$ partial pressure across the HDT reactor bed (—, simulation; ■, pilot data[11]).

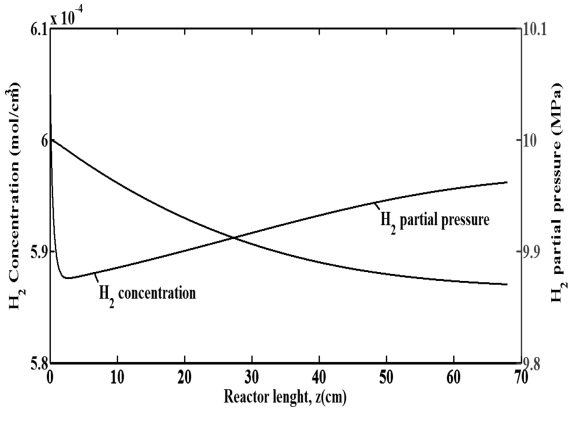


**Figure 3.** Simulation profiles of $H_2$ in gas and liquid phases across the HDT reactor bed.

output S concentration and $H_2S$ partial pressure by the experimental data.

Figure 4 shows the influence of the superficial gas velocity ($u_G$) on the output S concentration along the reactor bed in the range of 0.1−0.33 cm/s. The effect of the superficial gas velocity in the range of 0.1−0.18 cm/s is greater than this effect on 0.18−0.33 cm/s. Some reasons for this event can be related to catalyst coking, damaging, and others.[27] On the other hand,


dx.doi.org/10.1021/ef500701q | Energy Fuels 2014, 28, 4828−4834

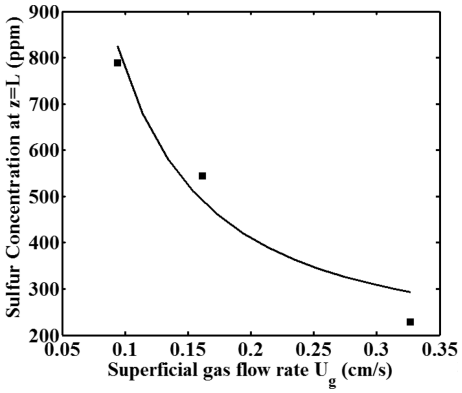


**Figure 4.** Effect of the gas/oil ratio at low liquid flow rate in the HDS reactor (—, simulation; ■, pilot data[11]).

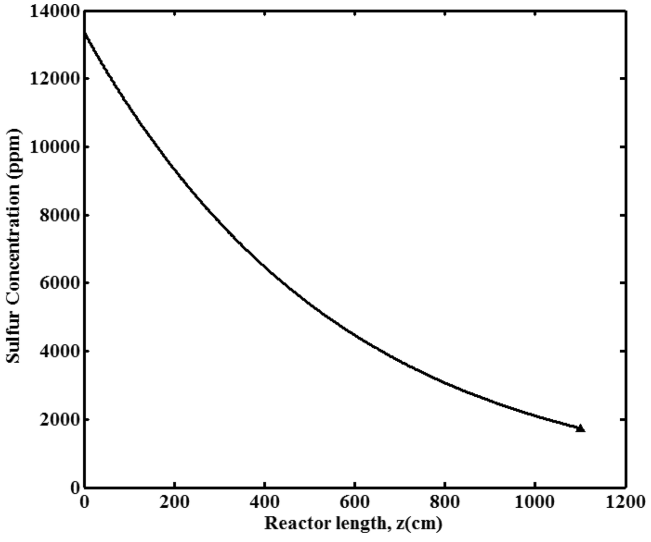


**Figure 5.** Predicted sulfur concentration profile in the HDT reactor (—, simulation; ▶, industrial data[27]).

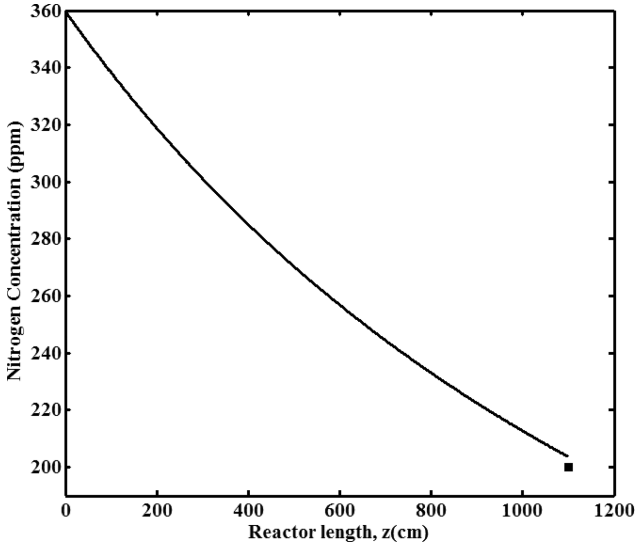


**Figure 6.** Predicted nitrogen concentration profile in the HDT reactor (—, simulation; ■, industrial data[27]).

appropriate operating conditions must be specified for reactor and catalyst optimal performance.

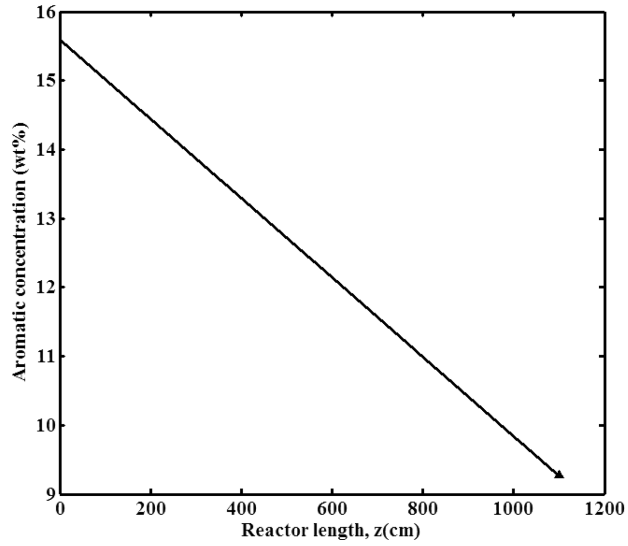


**Figure 7.** Predicted aromatic concentration profile in the HDT reactor (—, simulation; ▶, industrial data[27]).

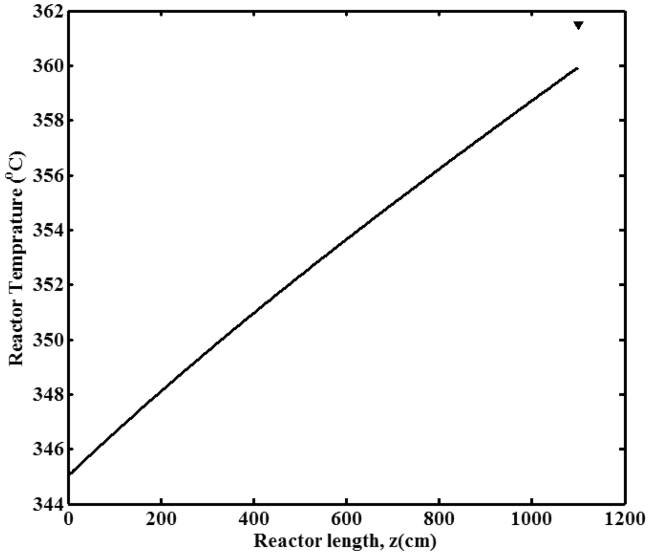


**Figure 8.** Predicted temperature profile across the HDT reactor bed (—, simulation; ▼, industrial data[27]).

Figures 5−7 show simulation profiles of sulfur, nitrogen, and aromatic concentrations across the industrial reactor, respectively. As observed, all of profiles demonstrate high reduction along the reactor bed and simulated results are very close to experimental data.

The predicted temperature profile along the HDT reactor bed is shown in Figure 8. The nonlinear trend of the temperature profile along the HDT reactor depends upon the applied type of reaction, kinetic model, and aromatic contents in the feed stream. Considering the applied HDA kinetic model, the reaction rate of HDA is approximately constant but high; therefore, the temperature profile through the reactor is linear because changes in the temperature according to eq 4 are constant along the reactor bed because of the rate equation of HDA, as expressed in eq 7. A similar trend can be found in Figure 8 of ref 15 and Figure 7 of ref 24. Also, as seen in Figure 5 of ref 25, the linear trend is almost dominant in beds 1 and 2 of the reactor, where the reaction rates are higher than bed 3, in which the trend of the temperature profile is almost nonlinear.


dx.doi.org/10.1021/ef500701q | Energy Fuels 2014, 28, 4828−4834

Table 4. Evaluation of the Presented HDT Model for the Product Sulfur Content of Different Feed Types

| feed type | API gravity | $S_{in}$ (mol/cm$^3$) | $S_{out,\ experiment}$ (mol/cm$^3$) | $S_{out,\ present\ model}$ (mol/cm$^3$) | reference |
|---|---|---|---|---|---|
| atmospheric residue | 5.4 | $1 \times 10^{-4}$ | $1.04 \times 10^{-5}$ | $1.04 \times 10^{-5}$ | 2 |
| Maya crude oil | 21 | $4.85 \times 10^{-5}$ | $1.86 \times 10^{-5}$ | $1.86 \times 10^{-5}$ | 21 |
| vacuum gas oil | 22 | $3.45 \times 10^{-5}$ | $8.63 \times 10^{-6}$ | $9.15 \times 10^{-6}$ | 6 |
| vacuum gas oil | 23 | $3.59 \times 10^{-5}$ | $9.17 \times 10^{-5}$ | $9.17 \times 10^{-5}$ | 14 |
| diesel fuel | 32 | $3.86 \times 10^{-5}$ | $4.81 \times 10^{-6}$ | $4.82 \times 10^{-6}$ | 27 |

The linear behavior of the temperature profile is directly related to the HDA reaction rate, because the HDA rate is much higher than HDS and HDN in the presented model. With regard to catalyst deactivation, the temperature profile can be decayed rapidly with time, as shown in refs 15 and 24.

The evaluation of the presented HDT model for the product sulfur content of various types of feed is presented in Table 4. A comparison of the predicted $S_{out}$ to those reported as real data[2,6,11,21,27] are very close. Thus, the presented model has the ability to simulate the sulfur content of the hydrotreated product as well as other component values, if required.

## 4. CONCLUSION

Modeling and simulation of the HDT trickle-bed reactor for both pilot and industrial scales is presented. Using Simulink has several advantages, such as being user-friendly, flexible, and efficient for the implemented method. Validation of this simulation shows good agreement with experiments. The component concentration gradient confirms the high ability of this simulation to predict the component profile through the reactor and the capacity of removal for this impurity content. Taking quench streams with regard to increased temperature along the reactor is inevitable. Controlling the operating parameters, such as a feed American Petroleum Institute (API) gravity, temperature, pressure, and LHSV, is one of the main concerns of each refinery because unexpected variations in each of these operating variables can cause serious damages to the plant. Simulink has high ability to control the operating conditions through entrance of the disturbances to the system, which can be the topic for the next studies in the future.

## AUTHOR INFORMATION

### Corresponding Author

*Telephone: 098511-8805149. E-mail: dashti@um.ac.ir.

### Notes

The authors declare no competing financial interest.

## NOMENCLATURE

HDA = hydrodearomatization
HDN = hydrodenitrogenation
HDS = hydrodesulfurization
$a_L$ = gas−liquid interfacial area (cm$^{-1}$)
$a_S$ = liquid−solid interfacial area (cm$^{-1}$)
$C_p^L$ = specific heat of the liquid phase (J g$^{-1}$ K$^{-1}$)
$C_i$ = molar concentration of the $i$ compound (mol/cm$^3$)
$D_i$ = molecular diffusivity of the $i$ compound (cm$^2$/s)
$E_A$ = activity energy (J/mol)
$G_L$ = superficial mass velocity (kg m$^{-2}$ s$^{-1}$)
$H_i$ = Henry's coefficient of the $i$ compound (MPa cm$^3$ mol$^{-1}$)
$k_{app}$ = apparent reaction rate constant
$k_j$ = reaction rate constant for the $j$ reaction
$k_i^L$ = gas−liquid mass-transfer coefficient for the $i$ compound (cm/s)
$k_i^S$ = liquid−solid mass-transfer coefficient for the $i$ compound (cm/s)
$K_{H_2S}$ = adsorption equilibrium constant of $H_2S$ (mol/cm$^3$)
$P$ = reactor pressure (MPa)
$p_i$ = partial pressure of the $i$ compound (MPa)
$r_j$ = reaction rate of the $j$ reaction (mol cm$^{-3}$ s$^{-1}$)
$T$ = reactor temperature (°C or K)
$u_G$ = gas superficial velocity (cm/s)
$u_L$ = liquid superficial velocity (cm/s)
$z$ = axial position of the reactor catalyst bed (cm)

### Greek Letters

$\Delta H_j$ = heat of the $j$ reaction (J/mol)
$\rho$ = density (g/cm$^3$)
$\mu_L$ = liquid viscosity (mPa s)
$\varepsilon$ = void fraction of the catalyst bed
$\eta_j$ = effectiveness factor of the $j$ reaction

### Subscripts

Ar = aromatic
$H_2$ = hydrogen
$H_2S$ = hydrogen sulfide
N = nitrogen
S = sulfur

### Superscripts

G = gas phase
L = liquid phase
S = solid phase

## REFERENCES

(1) Angeles, M. J.; Leyva, C.; Ancheyta, J.; Ramirez, S. A review of experimental procedures for heavy oil hydrocracking with dispersed catalyst. *Catal. Today* **2014**, *220−222*, 274−294.

(2) Alvarez, A.; Ancheyta, J. Modeling residue hydroprocessing in a multi-fixed-bed reactor system. *Appl. Catal., A* **2008**, *351* (2), 148−158.

(3) Ancheyta, J.; Sanchez, S.; Rodriguez, M. A. Kinetic modeling of hydrocracking of heavy oil fractions: A review. *Catal. Today* **2005**, *109*, 76−92.

(4) Adam, M.; Calemma, V.; Galimberti, F.; Gambaro, C.; Heiszowolf, J.; Ocone, R. Continuum lumping kinetics of complex reactive systems. *Chem. Eng. Sci.* **2012**, *76*, 154−164.

(5) Leyva, C.; Ancheyta, J.; Travert, A.; Mauge, F.; Mariey, L.; Ramirez, J.; Rana, M. S. Activity and surface properties of NiMo/$SiO_2$−$Al_2O_3$ catalysts for hydroprocessing of heavy oils. *Appl. Catal., A* **2012**, *425−426*, 1−12.

(6) Rodriguez, M. A.; Ancheyta, J. Modeling of hydrodesulfurization (HDS), hydrodenitrogenation (HDN), and the hydrogenation of aromatics (HDA) in a vacuum gas oil hydrotreater. *Energy Fuels* **2004**, *18*, 789−794.

(7) Bhaskar, M.; Valavarasu, G.; Sairam, B.; Balaraman, K. S.; Balu, K. Three-phase reactor model to simulate the performance of pilot-plant and industrial trickle-bed reactors sustaining hydrotreating reactions. *Ind. Eng. Chem. Res.* **2004**, *43*, 6654−6669.

(8) Rana, M. S.; Samano, V.; Ancheyta, J.; Diaz, J. A. I. A review of recent advances on process technologies for upgrading of heavy oils and residua. *Fuel* **2007**, *86*, 1216−1231.

(9) Murali, C.; Voolapalli, R. K.; Ravichander, N.; Gokak, D. T.; Choudary, N. V. Trickle-bed reactor model to simulate the performance of commercial diesel hydrotreating unit. *Fuel* **2007**, *86*, 1176−1184.
(10) Satterfield, C. N. Trickle-bed reactors. *AIChE J.* **1975**, *21*, 209−228.
(11) Korsten, H.; Hoffmann, U. Three-phase reactor model for hydrotreating in pilot trickle-bed reactors. *AIChE J.* **1996**, *42*, 1350−1360.
(12) Matos, E. M.; Guirardello, R. Modelling and simulation of the hydrocracking of heavy oil fractions. *Braz. J. Chem. Eng.* **2000**, *17*, 79−90.
(13) Chowdhury, R.; Pedernera, E.; Reimert, R. Trickle-bed reactor model for desulfurization and dearomatization of diesel. *AIChE J.* **2002**, *48*, 126−135.
(14) Marafi, A.; Fukase, M.; Al-Marri, M.; Stanislaus, A. A comparative study of the effect of catalyst type on hydrotreating kinetics of Kuwaiti atmospheric residue. *Energy Fuels* **2003**, *17*, 661−668.
(15) Mederos, F. S.; Rodríguez, M. A.; Ancheyta, J.; Arce, E. Dynamic modeling and simulation of catalytic hydrotreating reactors. *Energy Fuels* **2006**, *20*, 936−945.
(16) Alvarez, A.; Ancheyta, J. Effect of liquid quenching on hydroprocessing of heavy crude oils in a fixed-bed reactor system. *Ind. Eng. Chem. Res.* **2009**, *48*, 1228−1236.
(17) Alvarez, A.; Ancheyta, J.; Munoz, J. A. D. Modeling, simulation, and analysis of heavy oil hydroprocessing in fixed-bed reactors employing liquid quench streams. *Appl. Catal., A* **2009**, *361*, 1−12.
(18) Chen, J.; Mulgundmath, V.; Wang, N. Accounting for vapor−liquid equilibrium in the modeling and simulation of a commercial hydrotreating reactor. *Ind. Eng. Chem. Res.* **2011**, *50*, 1571−1579.
(19) Jarullah, A. T.; Mujtaba, I. M.; Wood, A. S. Kinetic model development and simulation of simultaneous hydrodenitrogenation and hydrodemetallization of crude oil in trickle-bed reactor. *Fuel* **2011**, *90*, 2165−2181.
(20) Alvarez, A.; Ancheyta, J. Transient behavior of residual oil front-end hydrodemetallization in a trickle-bed reactor. *Chem. Eng. J.* **2012**, *197*, 204−214.
(21) Rodriguez, M. A.; Elizalde, I.; Ancheyta, J. Modeling the performance of a bench-scale reactor sustaining HDS and HDM of heavy crude oil at moderate conditions. *Fuel* **2012**, *100*, 152−162.
(22) Jimenez, F.; Kafarov, V.; Nunez, M. Modeling of industrial reactor for hydrotreating of vacuum gas oils simultaneous hydrodesulfurization, hydrodenitrogenation and hydrodearomatization reactions. *Chem. Eng. J.* **2007**, *134*, 200−208.
(23) Mederos, F. S.; Ancheyta, J.; Elizalde, I. Dynamic modeling and simulation of hydrotreating of gas oil obtained from heavy crude oil. *Appl. Catal., A* **2012**, *425*−*426*, 13−27.
(24) Mederos, F. S.; Ancheyta, J. Mathematical modeling and simulation of hydrotreating reactors: Cocurrent versus countercurrent operations. *Appl. Catal., A* **2007**, *332*, 8−21.
(25) Jarullah, A. T.; Mujtaba, I. M.; Wood, A. S. Whole crude oil hydrotreating from small-scale laboratory pilot plant to large-scale trickle-bed reactor: Analysis of operational issues through modeling. *Energy Fuels* **2012**, *26*, 629−641.
(26) Jarullah, A. T.; Mujtaba, I. M.; Wood, A. S. Kinetic parameter estimation and simulation of trickle-bed reactor for hydrodesulfurization of crude oil. *Chem. Eng. Sci.* **2011**, *66*, 859−871.
(27) Barkhordari, A.; Fatemi, S.; Daneshpayeh, M. Kinetic modeling of industrial VGO hydrocracking in a life term of catalyst. *Proceedings of the 8th World Congress of Chemical Engineering (WCCE8)*; Montreal, Quebec, Canada, 2009; Paper 1013.
(28) Perry, R. H.; Green, D. W. *Perry's Chemical Engineers' Handbook*; McGraw-Hill: New York, 1999.
(29) Riazi, M. R. *Characterization and Properties of Petroleum Fractions*; ASTM International: West Conshohocken, PA, 2005.